Available online at www.sciencedirect.com
ScienceDirect
Journal of Hydrodynamics
2010,22(1):81-89
DOI: 10.1016/S1001-6058(09)60031-7
www.sciencedirect.com/science/journal/10016058

VISCOSITY EFFECTS ON THE BEHAVIOR OF A RISING BUBBLE*

WANG Han
Department of Mechanics and Engineering Science, Fudan University, Shanghai 200433, China,
E-mail: joycewanghan@yahoo.com.cn
ZHANG Zhen-yu
Department of Mathematics, Shanghai University of Finance and Economics, Shanghai 200433, China
YANG Yong-ming, ZHANG Hui-sheng
Department of Mechanics and Engineering Science, Fudan University, Shanghai 200433, China

(Received July 6, 2009, Revised November 9, 2009)

Abstract: In the incompressible fluid flow regime, without taking consideration of surface tension effects, the viscosity effects on the behavior of an initially spherical buoyancy-driven bubble rising in an infinite and initially stationary liquid are investigated numerically by the Volume Of Fluid (VOF) method. The ratio of the gas density to the liquid density is taken as 0.001, and the gas viscosity to the liquid viscosity is 0.01, which is close to the case of an air bubble rising in water. It is found by numerical experiments that there exist two critical Reynolds numbers Re_1 and Re_2, which are in between 30 and 50 and in between 10 and 30, respectively. As $Re > Re_1$ the bubble will have the transition to toroidal form, and the toroidal bubble will break down into two toroidal bubbles. In this case viscosity will damp the development of the liquid jet and delay the formation of the toroidal bubble. As $Re<Re_1$ the transition will not happen. As $Re_2 < Re < Re_1$, the bubble will split from its rim into a toroidal bubble and a spherical cap-like bubble, and as $Re<Re_2$ the splitting will not occur and the bubble can finally reach a stationary shape. With the decrease of the Reynolds number, the stationary shape changes from spherical-cap bubble with skirt to dimpled peach-like bubble. Before the bubble reaches its stationary shape the vortex structure in the flow field varies with time. The vortex structure corresponding to bubble stationary shape varies with the Reynolds number. It is also found that there exists another critical Reynolds number Re^* which is in between Re_1 and Re_2, and as $Re < Re^*$, after the bubble rises in an accelerating manner for a moment, it will rise with an almost constant speed, and the speed increases with increasing Reynolds number. As $Re > Re^*$, it will not rise with a constant speed. The mechanism of the above phenomena has been analyzed theoretically and numerically.

Key words: rising bubble, viscosity effects, buoyancy force, Volume Of Fluid (VOF) method

1. Introduction

Multifluid systems play an important role in many natural and industrial processes such as combustion, petroleum refining, chemical engineering and cleaning. The rising of a buoyancy- driven bubbles in a liquid is one of the typical dynamics of multifluid systems. A sound understanding of the fundamentals of the rising bubble is crucial in a variety of practical applications ranging from the rise of steam in boiler tubes to gas bubbles in oil wells. It is difficult to study the mechanism of the bubble behavior through pure theoretical analysis because of the strong nonlinearity accompanied by large deformations of bubbles. As a result, approximate

* Project supported by the National Natural Science Foundation of China (Grant Nos.10672043, 10272032).
Biography: WANG Han (1983-), Female, Manchu, Ph. D. Candidate
Corresponding author: YANG Yong-ming,
E-mail: yangym@fudan.edu.cn

theoretical solutions have been obtained in the limitation of very small bubble deformations for either high[1] or low[2] Reynolds numbers. The well-known analysis in Ref.[3] related the rising speed to the radius of curvature of the bubble at the forward stagnation point, but the overall spherical-cap shape was assumed *a prior* rather than being determined as a part of a full solution.

Up to now, the large deformations of the bubble have been studied mainly with experimental approach and numerical simulation. The experimental approach is the most direct and original one to find new phenomena and to explore the associated mechanisms. Early observation works have been done by many authors[4-7]. However, it is rather difficult to measure the flow pattern and pressure distribution within the bubble and its surrounding liquid while it is rising and deforming. Moreover, the correlations obtained by experiments are based on a limited number of liquid/gas systems. On the other hand, numerical approach can overcome these drawbacks and provide an effective and convenient way to solve multifluid flow problems.

The numerical simulation methods for multifluid problems can mainly be divided into two categories. One is the kind of boundary integral methods[8], which only needs to arrange the grids on the bubble surfaces and thus reduces the dimensions of the problem by one, so that the computational amounts are, compared to the other kinds of methods mentioned below, reduced considerably. These methods can simulate the bubble shape with high resolution and are easy to implement simulation of surface tension effects accurately. The boundary conditions of the flow field at infinity can be satisfied exactly in these methods. However, this kind of methods is difficult to simulate the topological changes of the flow field such as the transition from single-connected domain to multi-connected domain, bubble merging and break, etc.. It is also difficult for these methods to model the viscous effects of the fluids for flows with moderate Reynolds numbers, and is not convenient to give the velocity and pressure distributions.

The other category is the kind of methods based on the full-flow-field solutions such as the body-fitted grids methods[9], front tracking methods[10-12], level set methods[13-15], Volume Of Fluid (VOF) methods[13,16-18], Coupled Level Set and VOF (CLSVOF) methods[19], etc.. These methods are easy to give the detailed velocity and pressure distributions as a direct result of the computation, and can simulate viscosity effects on the flow, and some of them can easily track the topological changes of interfaces.

Among all those articles mentioned above, some of them[19] focused mainly on the numerical method and only gave the computed results but neglect the analysis of the mechanism of bubbles behavior. Others[11,17] conducted both simulation and mechanism analysis, nevertheless in these analyses, the influences of several factors such as the density ratio, the viscosity ratio, the Reynolds number and the Weber number were mixed, and the fluid mechanics and the bubble behavior were not combined specifically, so that these analyses of the parametrical effects are not precise enough.

We are trying to analyze numerically the deformation mechanism of initially spherical bubbles or drops during their buoyancy-driven motion (rising or falling) in another infinite and initially stationary fluid by VOF method. The Weber number, the Reynolds number, the density ratio, and the viscosity ratio are the crucial dimensionless parameters in controling the flow. In order to make the analysis proper, at first we should study the effects of the four factors separately, and then study their combined effects, so that we can fully understand the associated mechanisms. In Ref.[20] we have improved the VOF method which can appropriately simulate the motion and deformation of a buoyancy-driven bubble or drop with taking consideration of the effects of the four parameters mentioned above, and analyzed the mechanism of the generation of the liquid jet during the bubble or drop motion without taking considering the surface tension and viscosity effects (therefore the effects of the viscosity ratio was automatically neglected). Hence, in that case, the only dimensionless parameter that will affect the flow pattern is the density ratio of the two fluids, and the bubble or drop is only driven by the inertia force. In our simulation, we found that with the increase of the density ratio, the evolution of the bubble deformation becomes gradually slower due to larger resistance, and compared with the bubble, the resistance to the deformation of the drop is larger due to its larger density ratio, where the density ratio is defined as the ratio of the fluid density inside the surface to the fluid density outside the surface. In Ref.[21] we studied the surface tension effects of the rising bubble and we found that there are four critical Weber numbers which distinguish five kinds of bubble behaviors.

As a follow-up of Refs.[20] and [21], this article will investigate numerically the viscosity effects on the behavior of a rising bubble with the VOF method. The viscosity effects will be important as the Reynolds number *Re* is small, or as flow separation occurs. An example of the second case is that when a bubble rises in liquid with a stationary shape, behind the bubble the boundary layer will separate from the bubble surface, and the viscosity effect will be dominant there. Ref.[22] studied the effect of viscosity on jet formation and evolution for a cavitation bubble collapsing near a solid boundary by the finite volume and MAC scheme.

The remaining of this article is arranged as

follows. Section 2 gives the governing equations. Section 3 shows the numerical results and the mechanism analysis. Section 4 outlines the conclusions and discussion.

2. Governing equations

We study the buoyancy-driven motion of an axisymmetric bubble with the surface S in an infinite and initially stationary fluid. Let the fluids outside and inside S be marked by 1 and 2 respectively. The two fluids are assumed to be immiscible and incompressible. Let ρ and μ be the fluid density and viscosity respectively, and C be the ratio of the volume of fluid 1 in a cell to the volume of the cell (C is called the color function). Assume l_0, $u_0=\sqrt{gl_0}$, $t_0=l_0/u_0$, $p_0=\rho_1 u_0^2$, ρ_1 and μ_1 to be the reference quantities of length, velocity, time, pressure, density, and viscosity, respectively, and introduce the following dimensionless quantities

$$\bar{r}=r/l_0,\ \bar{z}=z/l_0,\ \bar{t}=t/t_0,\ \bar{u}=u/u_0,$$

$$\bar{v}=v/u_0,\ \bar{p}=p/p_0,\ \bar{\rho}=\rho/\rho_1,$$

$$\bar{\mu}=\mu/\mu_1$$

Then we can get the dimensionless governing equations for the flow problem. In the above and following expressions, r and z are respectively the radial and axial coordinates, t is the time variable, u and v are respectively the r- and z-components of the velocity, p is the pressure, g is the acceleration due to gravity, σ is the surface tension between fluids 1 and 2, α is the total curvature of S, $\delta(S)$ is the Dirac δ-function with sources distributed on S, and n_r and n_z are respectively the r- and z- components of the unit normal of S. If we drop the bar "-" over each dimensionless quantity, then the dimensionless governing equations are

$$\frac{1}{r}\frac{\partial(ru)}{\partial r}+\frac{\partial v}{\partial z}=0 \tag{1}$$

$$\frac{\partial u}{\partial t}+\frac{1}{r}\frac{\partial(ru^2)}{\partial r}+\frac{\partial(uv)}{\partial z}=\frac{1}{We\rho}\alpha\delta(S)n_r-$$

$$\frac{1}{\rho}\frac{\partial p}{\partial r}+\frac{1}{Re\rho}\left\{\frac{1}{r}\frac{\partial}{\partial r}\left(2\mu r\frac{\partial u}{\partial r}\right)+\frac{\partial}{\partial z}\bullet\right.$$

$$\left.\left[\mu\left(\frac{\partial u}{\partial z}+\frac{\partial v}{\partial r}\right)\right]-\frac{2\mu u}{r^2}\right\} \tag{2}$$

$$\frac{\partial v}{\partial t}+\frac{1}{r}\frac{\partial(ruv)}{\partial r}+\frac{\partial(v^2)}{\partial z}=\frac{1}{We\rho}\alpha\delta(S)n_z-$$

$$\frac{1}{\rho}\frac{\partial p}{\partial z}+\frac{1}{Re\rho}\left\{\frac{1}{r}\frac{\partial}{\partial r}\left[r\mu\left(\frac{\partial u}{\partial z}+\frac{\partial v}{\partial r}\right)\right]+\right.$$

$$\left.\frac{\partial}{\partial z}\left(2\mu\frac{\partial v}{\partial z}\right)\right\} \tag{3}$$

$$\frac{\partial C}{\partial t}+u\frac{\partial C}{\partial r}+v\frac{\partial C}{\partial z}=0 \tag{4}$$

$$\rho=\lambda+C(1-\lambda) \tag{5}$$

$$\mu=\beta+C(1-\beta) \tag{6}$$

where the dimensionless parameters λ, β, Fr, Re and We, are respectively the density ratio, viscosity ratio, Froude number, Reynolds number and Weber number, which are defined by

$$\lambda=\frac{\rho_2}{\rho_1},\ \beta=\frac{\mu_2}{\mu_1},\ Fr=\frac{u_0^2}{gl_0},$$

$$Re=\frac{\rho_1 u_0 l_0}{\mu_1},\ We=\frac{\rho_1 u_0^2 l_0}{\sigma} \tag{7}$$

Because in this article we take $u_0=\sqrt{gl_0}$, so we always have $Fr=1$ and $We=\rho_1 g l_0^2/\sigma$ (in this case We is called the Bond number B).

At infinity the velocity is set to be zero and the pressure to be the stationary fluid pressure. In the following computations, by use of the axisymmetric property of the fluid flow, the grid points at the symmetric axis can be treated as inner grid points. The governing equations were solved numerically by the method given in Ref.[20].

3. Numerical results

We will study the buoyancy-driven motion of an initially spherical bubble in initially stationary infinite fluid. In the normalization, the reference length and

velocity are taken to be R and $\sqrt{gR}$ respectively, where R is the radius of the bubble at $t=0$. Therefore, in the dimensionless system, the radius of the bubble at $t=0$ is always 1, and the Froude number Fr is also always 1. In this article, all of the numerical results are in dimensionless form.

To solve our flow problem in infinite domain, it is necessary to truncate the flow field to a finite domain: $0 \le r \le r_{\max}$ and $z_l \le z \le z_u$. Numerical experiments with $\Delta r = \Delta z = 0.1$ show that when $r_{\max} \ge 3$ and d_l, d_u, the distances from the bubble to z_l, z_u, are greater than or equal to 2, the numerical results for the evolution of the bubble only have small differences for different $r_{\max}$, z_l and z_u. In the computations of this article we take $r_{\max} = 8$ and take z_l and z_u so that $d_l \ge 7$ and $d_u \ge 7$ are ensured during the evolution of the bubble. Numerical experiments also show that the numerical results with $\Delta r = \Delta z = 0.1$ and those with $\Delta r = \Delta z = 0.2$ have distinguishable differences, but the numerical results with $\Delta r = \Delta z = 0.1$ and those with $\Delta r = \Delta z = 0.05$ only have small differences. Thus in the computations of this article, we set $\Delta r = \Delta z = 0.1$. In all of the computations, $\Delta t = 0.001$ is taken.

To demonstrate the correctness and validity of our method, Fig.1 shows the comparison of our numerical results (the right) with the experimental results (the left) of Hnat and Buckmaster (Fig.1(a) in Ref.[6] for the case of $\lambda = 0.0011$, $\beta = 0.0085$, $Re = 9.8$, $We = 7.6$ and $Fr = 0.76$). Figure 6 in Ref.[9] and Fig.17 in Ref.[23] also gave similar comparisons. The terminal rise velocity measured in Ref.[6] is 0.215 m/s, and the terminal rise velocity computed by our method is 0.232 m/s. It can be seen that the agreements in the stationary shape of bubble and the flow pattern are good.

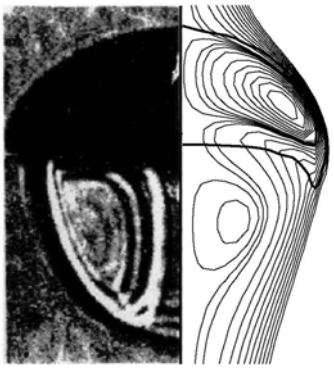

Fig.1 Stationary shape of bubble and the corresponding flow pattern with $\lambda = 0.0011$, $\beta = 0.0085$, $Re = 9.8$, $We = 7.6$ and $Fr = 0.76$. The left is the results in Ref.[6] and the right is the present numerical results

For the case of $\lambda = 0.001$, $Re = \infty$, $We = 10$ and $Fr = 1$, Fig.2(a) gives the evolution of an initially spherical gas bubble in a liquid by our method. Figure 2(b) shows the corresponding results from Fig.10 in Ref.[24] by the level set method. Very good agreement is achieved. Another comparison with the numerical results in Ref.[24] is given in Ref.[21], which also verifies the validity of our method.

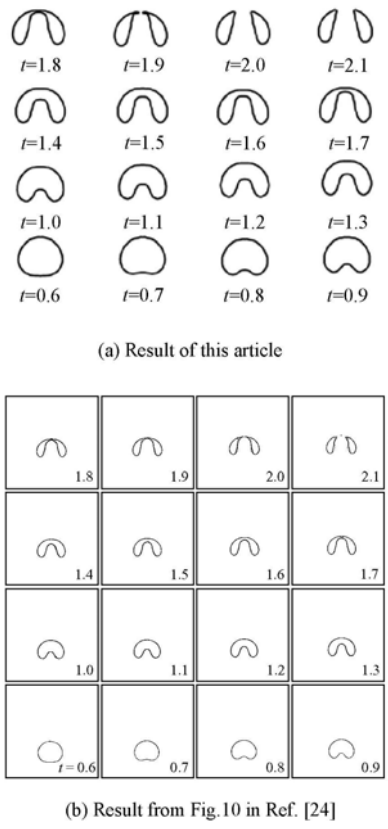

Fig.2 Evolution of an initially spherical gas bubble in a liquid with $\lambda = 0.001$, $Re = \infty$, $We = 10$ and $Fr = 1$

It has been known that in the framework of potential flow theory, without the consideration of surface tension effects, due to the action of the inertial force, i.e., the gradient of the pressure p_{df} that causes the bubble to deform, where $p_{df} = p - p_{st}$ and p_{st} is the stationery fluid pressure, (see Ref.[20]), two liquid jets will form during the rising of the bubble. One is large and behind the bubble, the other is much smaller and ahead of the bubble, and the development of the two jets will make the bubble toroidal[20].

Now we investigate the viscosity effects on the behavior of a rising bubble. It should be noted that for an initially spherical bubble viscosity will dissipate the flow energy and thus will resist the formation and development of the liquid jets. Therefore whether the

liquid jets will form or not, and how they will develop if they form and whether they will cause the bubble to become toroidal, will depend on the relative importance of the inertial force and the viscosity. In all of the computations, the density ratio λ is set to be 0.001 and the viscosity ratio β to be 0.01, which is close to the case of an air bubble rising in water.

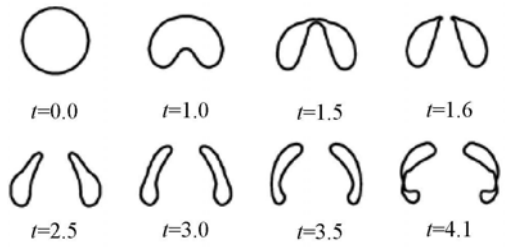

Fig.3(a) Evolution of a gas bubble in liquid with $\lambda = 0.001$, $\beta = 0.01$, $Re = 200$, $We = \infty$ and $Fr = 1$

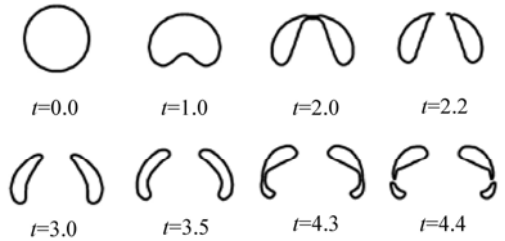

Fig.3(b) Evolution of a gas bubble in liquid with $\lambda = 0.001$, $\beta = 0.01$, $Re = 50$, $We = \infty$ and $Fr = 1$

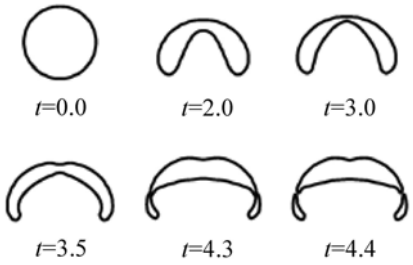

Fig.3(c) Evolution of a gas bubble in liquid with $\lambda = 0.001$, $\beta = 0.01$, $Re = 30$, $We = \infty$ and $Fr = 1$

For $\lambda = 0.001$, $\beta = 0.01$, $We = \infty$ and $Fr = 1$, Figs.3(a)-3(e) give the evolutions of the bubble with $Re = 200$, 50, 30, 20, and 10 respectively. The number below each picture indicates its corresponding time. It can be seen that there exist two critical Reynolds numbers Re_1 and Re_2, which are in between 30 and 50 and in between 10 and 20, respectively. When $Re > Re_1$, the bubble will undergo the transition to the toroidal form, and the toroidal bubble will break down into two toroidal bubbles. When $Re < Re_1$, the transition will not happen. When $Re_2 < Re < Re_1$, the bubble will split from its rim into a toroidal bubble and a spherical cap-like bubble, and when $Re < Re_2$, the splitting will not occur.

It can be seen from Figs.3(a)-3(b) that in the case of $Re > Re_1$, after the toroidal bubble forms, it moves outward due to the action of the lift, and its cross-section area decreases in order to keep the conservation of its volume. As was analyzed in Ref.[20], the lift is induced by the co-action of the upward motion of the bubble and the circulation around its cross section. The top part of its cross section is sharp and then the top of the toroidal bubble moves inward. Afterwards the lower part of the bubble becomes thinner and thinner. At the same time, its upper part becomes a little fatter, its cross section continuously elongates upward and its top continuously moves inward. Then the lower middle part of the cross section becomes thinner and thinner, and at last the toroidal bubble breaks down into two toroidal bubbles. The above phenomena are similar to those in the inviscid fluid flow case and have been analyzed in Ref.[21].

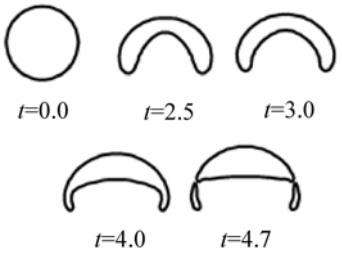

Fig.3(d) Evolution of a gas bubble in liquid with $\lambda = 0.001$, $\beta = 0.01$, $Re = 20$, $We = \infty$ and $Fr = 1$

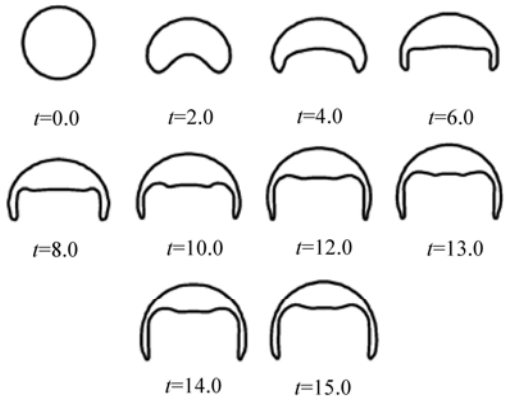

Fig.3(e) Evolution of a gas bubble in liquid with $\lambda = 0.001$, $\beta = 0.01$, $Re = 10$, $We = \infty$ and $Fr = 1$

Now we analyze the evolution mechanism of the liquid jets. As was pointed out in Ref.[20], the pressure p_{df} will cause the bubble to deform. First we investigate the generation and development of the liquid jet in the framework of inviscid flow and without taking consideration of surface tension effects.

As was analyzed in Ref.[20], when the bubble rises for a time the flow around the bubble collides with each other at the rear of the bubble and is blocked there. By Bernoulli's theorem, a large maximum of p_{df} with very large pressure gradient will be generated behind the bubble which will push the liquid behind the bubble to move with a large acceleration and thus a liquid jet forms and develops. The propagation of the large pressure gradient behind the bubble causes the generation and development of the liquid jet. As the liquid jet develops, the jet becomes longer and longer (thus the inertia of the jet becomes larger and larger), the pressure gradient within the jet decreases. Figure 4 gives the pressure distribution of p_{df} with $\lambda=0.001$, $\beta=0.01$, $Re=\infty$, $We=\infty$ and $Fr=1$ at $t=0.8$ and $t=1.4$. It can be seen that when the tip of the jet is below the bubble centroid ($t=0.8$), the acceleration in the jet is upward, and when the tip of the jet is above the bubble centroid ($t=1.4$), the acceleration in the bottom of the jet is upward but the acceleration at the top of the jet is downward. Figure 5 gives the vertical velocities *v* at the mid points of the upper and lower surfaces of the bubble for the same case as indicated in Fig.4. It can be seen that at early time the two points have the same vertical velocity. Then the liquid jet accelerates first and then decelerates until the toroidal bubble forms, and the velocity at the top surface of the bubble is nearly constant. Even if just before jet impact, the tip velocity of jet is still much higher than the velocity at the top surface of the bubble, which causes a circulation around the toroidal bubble. Therefore at the later time the deceleration of the liquid jet is caused not only by the surface tension, but also by the inertia force, which revises the analysis of Ref.[17]. It also illustrates that in order to understand the mechanism of the bubble behavior, it is necessary to study the effects of the dimensionless parameters separately first.

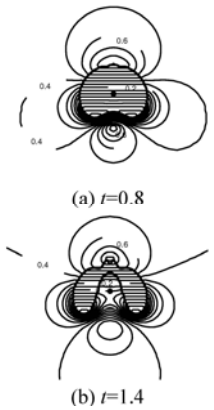

Fig.4 Pressure distribution of a gas bubble in liquid with $\lambda=0.001$, $\beta=0.01$, $Re=\infty$, $We=\infty$ and $Fr=1$ when $t=0.8$ and $t=1.4$

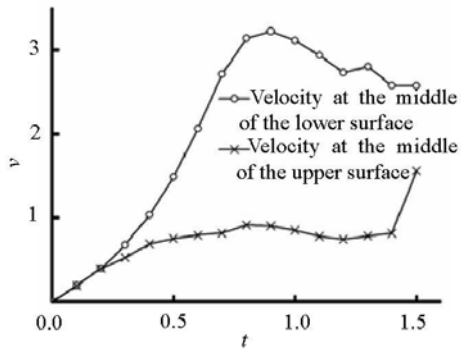

Fig.5 Vertical velocities at the mid points of the upper and lower surfaces of the bubble for $\lambda=0.001$, $\beta=0.01$, $Re=\infty$, $We=\infty$ and $Fr=1$

For $\lambda=0.001$, $\beta=0.01$, $We=\infty$ and $Fr=1$, Fig.6 gives the detailed evolution of the bubble with $Re=\infty$, 100 and 50 respectively. It can be seen that the viscosity will damp the development of the liquid jet and delay the formation of the toroidal bubble.

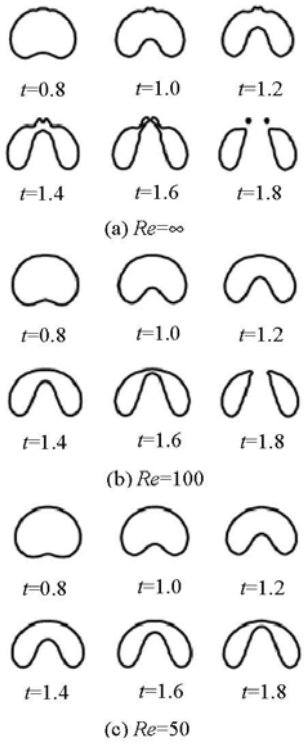

Fig.6 Evolution of a gas bubble in liquid with $\lambda=0.001$, $\beta=0.01$, $We=\infty$ and $Fr=1$

It can be seen from Figs.3(c)-3(e) that when viscosity is strong enough ($Re<Re_1$), the liquid jet will be so weak that the transition to toroidal bubble will not occur. However, when $Re_2<Re<Re_1$ the upper part of the bubble becomes thicker and thicker, and the lower part becomes thinner and thinner and at

last a toroidal bubble will be split from the rim of the bubble. When $Re < Re_2$ the splitting will not happen and the bubble will finally have a stationary form. Now we analyze the mechanism of the above phenomena. As was analyzed above, during the later time of the jet development the acceleration at the top of the jet is downward so that the bubble is thickened vertically. Figure 7 shows the flow velocity distribution at $t = 3.8$ for the case indicated in Fig.3(c). It can be seen that there exists a velocity circulation around the lower part of the bubble, which will finally cause the splitting as analyzed in Ref.[21].

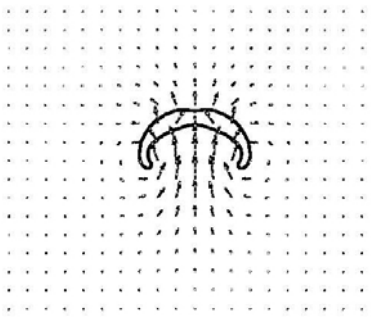

Fig.7 Velocity distribution at $t = 3.8$ for the case indicated in Fig.3(c)

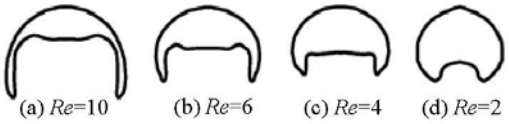

Fig.8 The final stationary shape of a gas bubble in liquid with different Reynolds numbers for $\lambda = 0.001$, $\beta = 0.01$, $We = \infty$ and $Fr = 1$

It can be seen from Fig.3(e) that in the case where $Re < Re_2$, the transition to toroidal bubble will not occur and after the bubble evolutes for a while, its rim stretches downward and finally it reaches a stationary shape–a spherical-cap with skirt. For $\lambda = 0.001$, $\beta = 0.01$, $We = \infty$ and $Fr = 1$, Fig.8 gives the final stationary shape of the rising bubble with $Re = 10$, 6, 4 and 2. It can be seen that with the decrease of the Reynolds number, the stationary shape changes from spherical-cap bubble with a skirt to dimpled peach-like bubble. These are in good agreement with the results for large Weber number cases given in Ref.[25]. It should be noted that even when $Re = 2$ the corresponding bubble stationary shape is still far away from spherical, which indicates that when $Re < Re_2$ fluid viscosity will help a rising bubble reach a stationary shape but not help it to become spherical, and only when both the Reynolds number and the Weber number are low enough the bubble can be easy to reach a stationary spherical shape.

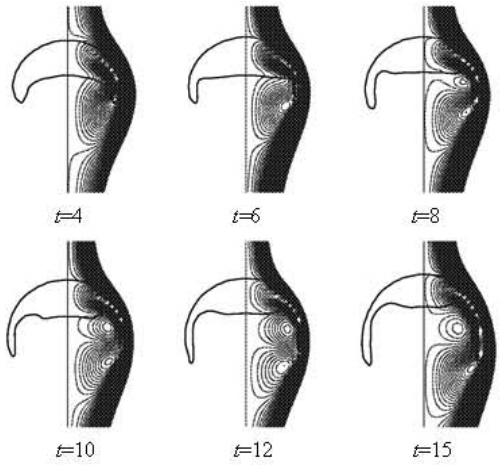

Fig.9 The evolution of the flow pattern of the rising bubble described by streamlines for the case indicated in Fig.3(e)

Figure 9 shows the evolution of the flow pattern described by streamlines for the case indicated in Fig.3(e). It can be seen that after the bubble evolves for a while, there is only one main vortex ring in the flow field ($t = 4$). Then it splits into two vortex rings, one is in the bubble and the other is in the wake of the bubble ($t = 6$). Then there appear three vortex rings, one is in the bubble, the other two counter-rotating vortex rings are in the wake of the bubble. Therefore before the bubble reaches its stationary shape, the vortex structure in the flow field varies with time.

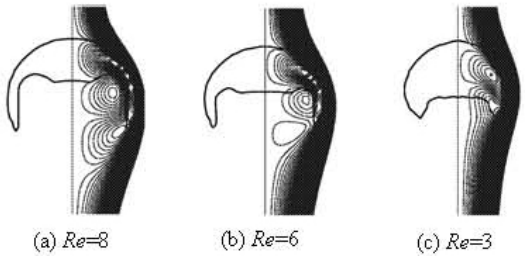

Fig.10 The stationary shape and the corresponding flow pattern of the rising bubble for $\lambda = 0.001$, $\beta = 0.01$, $We = \infty$ and $Fr = 1$

For $\lambda = 0.001$, $\beta = 0.01$, $We = \infty$ and $Fr = 1$, Fig.10 gives the final stationary shape and the corresponding flow pattern of the rising bubble with $Re = 8$, 6 and 3. It can be seen that when $Re = 8$, there are three vortex rings similar to the case in Fig.9, and the wake is larger than the frontal part of the bubble. When $Re = 6$, the lowest vortex ring becomes weak and the middle vortex ring moves

upward and near the skirt, and the wake is smaller than the bubble. When $Re = 3$, there is no vortex ring in the wake but only one inside the bubble. The above phenomena are in good agreement with the results of Ref.[7] for higher Weber numbers. Moreover, if the stationary shape of the bubble is skirted, the toroidal wake extends somewhat beyond the lower edge of the skirt, which can be also seen in Ref.[7].

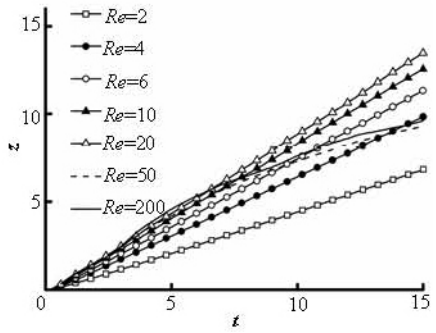

Fig.11 Evolution of the centroid position of a gas bubble for different Reynolds numbers with $\lambda = 0.001$, $\beta = 0.01$, $We = \infty$ and $Fr = 1$

When $\lambda = 0.001$, $\beta = 0.01$, $We = \infty$ and $Fr = 1$, Fig.11 shows the evolution of the centroid position of a gas bubble for different Reynolds numbers. It can be seen that there exists another critical Reynolds number Re^* which is in between Re_1 and Re_2, and when $Re < Re^*$, after the bubble rises in an accelerating way for a moment, it will rise with an almost constant speed, and the speed increases with increasing Reynolds number. When $Re > Re^*$, it will not rise with a constant speed. Now we analyze the mechanism of the phenomena. When $\lambda = 0.001$, $\beta = 0.01$, $We = \infty$ and $Fr = 1$, we conducted long time computation ($t \le 15$) for the evolution of the bubble shape, and the velocity and pressure distributions with $Re = \infty$, 200, 100, 50, 40, 30, 20, 15, 10, 9, 8, 7, 6, 5, 4, 3 and 2 respectively, although we only give part of the results for some selected Reynolds numbers because of the limitation of the article volume. We found that when $Re > Re^*$, the shape of the bubble keeps changing appreciably so that it can not rise with a constant speed. When $Re_2 \le Re < Re^*$, the large deformation of the bubble only lasts for a moment, and then the deformation has a small effect on the motion of the bubble centroid so that the bubble can rise with a nearly constant speed. When $Re < Re_2$, at early time the bubble rises with a nearly constant speed, as analyzed in the case of $Re_2 \le Re < Re^*$, and after it reaches a stationary shape, the viscous drag will balance the buoyancy force and it will rise with a constant speed, which is like a solid body rising in viscous liquid.

4. Conclusions and discussion

In the regime of incompressible fluid flow without taking consideration of surface tension effects, the viscosity effects on the behavior of an initially spherical buoyancy-driven bubble rising in an infinite and initially stationary liquid have been investigated numerically by the VOF method. The ratio of the gas density to the liquid density is 0.001, and the ratio of the gas viscosity to the liquid viscosity is 0.01. The validity of the numerical method has been checked. It is found by numerical experiments that there exist two critical Reynolds numbers Re_1 and Re_2, which are in between 30 and 50 and in between 10 and 20, respectively. When $Re > Re_1$ the bubble will undergo the transition to toroidal form, and the toroidal bubble will break down into two toroidal bubbles. In this case, viscosity will damp the development of the liquid jet and delay the formation of the toroidal bubble. When $Re < Re_1$ the transition will not happen. When $Re_2 < Re < Re_1$, the bubble will split from its rim into a toroidal bubble and a spherical cap-like bubble, and when $Re < Re_2$ the splitting will not occur and the bubble can finally reach a stationary shape. With the decrease of the Reynolds number, the stationary shape changes from spherical-cap bubble with a skirt to dimpled peach-like bubble. Before the bubble reaches its stationary shape the vortex structure in the flow field varies with time. The vortex structure corresponding to bubble steady shape varies with the Reynolds number. It is also found that there exists another critical Reynolds number Re^* which is in between Re_1 and Re_2, and when $Re < Re^*$, after the bubble rises in an accelerating way for a moment, it will rise with an almost constant speed, and the speed increases with increasing Reynolds number. When $Re > Re^*$, it will not rise with a constant speed. The mechanism of the above phenomena has been analyzed theoretically and numerically.

From Ref.[21] and this article we can see that the surface tension and fluid viscosity can both resist the development of the liquid jet and delay or even prevent the formation of the toroidal bubble, although their mechanisms are different: the surface tension will resist the increase of bubble surface energy, whereas the fluid viscosity will dissipate the flow kinematic energy. We can also see that when the Reynolds number is low enough, the rising bubble will be easy to reach a stationary shape which is far away from spherical, i.e., in this case the viscosity will

help the bubble to reach a stationary shape but not help it to become spherical. When the Weber number is very low the rising bubble will not be easy to reach a stationary shape but will oscillate near a spherical shape, i.e., in this case the surface tension will help the bubble to become spherical but not help it to reach a stationary shape due to the surface oscillation induced by the surface tension. Only when both the Reynolds number and the Weber number are low enough, the bubble can be easy to reach a stationary spherical shape. Due to the coupled action of the inertial force and the surface tension force or the viscosity force, when the Weber number or the Reynolds number is high enough, at very late time, the bubble will split many times. The mechanism of this phenomenon is not very clear yet and needs further study.

ACKNOWLEDGEMENT

This work was supported by the Fudan University Graduate Innovation Fund No. 7.

References

[1] MOORE D. W. The rise of a gas bubble in a viscous liquid[J]. **J. Fluid Mech.,** 1959, 6: 113-130.

[2] TAYLOR T. D., ACRIVOS A. On the deformation and drag of a falling viscous drop at low Reynolds number[J]. **J. Fluid Mech.,** 1964, 18: 466-476.

[3] DAVIES R. M., TAYLOR F. I. The mechanics of large bubbles rising through extended liquids and through liquids in tubes[J]. **Proc. R. Soc. Lond. A,** 1950, 200: 375-390.

[4] WALTERS J. K., DAVIDSON J. F. The initial motion of a gas bubble formed in an inviscid liquid Part 1. The two-dimensional bubble[J]. **J. Fluid Mech.,** 1962, 12: 408-416.

[5] WALTERS J. K., DAVIDSON J. F. The initial motion of a gas bubble formed in an inviscid liquid Part 2. The three-dimensional bubble and the toroidal bubble[J]. **J. Fluid Mech.,** 1963, 17: 321-336.

[6] HNAT J. G., BUCKMASTER J. D. Spherical cap bubbles and skirt formation[J]. **Phys. Fluids,** 1976, 19(2): 182-194.

[7] BHAGA D., WEBER M. E. Bubbles in viscous liquids: Shapes, wakes and velocities[J]. **J. Fluid Mech.,** 1981, 105: 61-65.

[8] ZHANG Y. L., YEO K. S. and KHOO B. C. et al. 3D jet impact and toroidal bubbles[J]. **J. Comp. Phys.,** 2001, 166(2): 336-360.

[9] RYSKIN G., LEAL L. G. Numerical solution of free-boundary problems in fluid mechanics. Part 2. Buoyancy-driven motion of a gas bubble through a quiescent liquid[J]. **J. Fluid Mech.,** 1984, 148: 19-35.

[10] UNVERDI S. O., TRYGGVASON G. A front-tracking method for viscous, incompressible, multi-fluid flows[J]. **J. Comp. Phys.,** 1992, 100: 25-37.

[11] HUA J. S., JING L. Numerical simulation of bubble rising in viscous fluid[J]. **J. Comp. Phys.,** 2007, 222: 769-795.

[12] CHEN Hui, LI Sheng-cai and ZUO Zhi-gang et al. Direct numerical simulation of bubble-cluster's dynamic characteristics[J]. **Journal of Hydrodynamics,** 2008, 20(6): 689-695.

[13] LIU Ru-xun, SHU Chi-wang. **Some new methods in computational fluid dynamics**[M]. Beijing: Chinese Academic Press, 2003(in Chinese).

[14] HUANG Jun-tao, ZHANG Hui-sheng. A level set method for simulation of rising bubble[J]. **Journal of Hydrodynamics, Ser. B,** 2004, 16(4): 379-385.

[15] HUANG Jun-tao, ZHANG Hui- sheng. Level set method for numerical simulation of a cavitation bubble collapsing near a rigid wall[J]. **Journal of Hydrodynamics, Ser. B,** 2005, 17(6): 647-653.

[16] CHEN Xin, LU Chuan- jing. Numerical simulation of ventilated cavitating flow around a 2D foil[J]. **Journal of Hydrodynamics, Ser. B,** 2005, 17(5): 607-614.

[17] CHEN L., SURESH V. The development of a bubble rising in a viscous liquid[J]. **J. Fluid Mech.,** 1999, 387: 61-96.

[18] LU Lin, LI Yu-cheng and TENG Bin et al. Numerical simulation of turbulent free surface flow over obstruction[J]. **Journal of Hydrodynamics,** 2008, 20(4): 414-423.

[19] SUSSMAN M. A second order coupled level set and volume-of-fluid method for computing growth and collapse of vapor bubbles[J]. **J. Comp. Phys.,** 2003, 187: 110-136.

[20] WANG Han, ZHANG Zheng-yu and YANG Yong-ming et al. Numerical investigation of the deformation mechanism of a bubble or a drop rising or falling in another fluid[J]. **Chin. Phys. B,** 2008, 17(10): 3847-3855.

[21] WANG Han, ZHANG Zheng-yu and YANG Yong-ming et al. Surface tension effects on the behavior of a rising bubble driven by buoyancy force[J]. **Chin. Phys. B,** 2010, 19(2): 026801-1-026801-9.

[22] POPINET S., ZALESKI S. Bubble collapse near a solid boundary: A numerical study of the influence of viscosity[J]. **J. Fluid Mech.,** 2002, 464: 137-163.

[23] SUSSMAN M., SMITH K. M. and HUSSAINI M. Y. et al. A sharp interface method for incompressible two-phase flows[J]. **J. Comp. Phys.,** 2007, 221: 469-505.

[24] SUSSMAN M., SMEREKA P. Axisymmetric free boundary problems[J]. **J. Fluid Mech.,** 1997, 341: 269-294.

[25] CLIFT R., GRACE J. R. and WEBER M. E. **Bubbles, drops, and particles**[M]. New York: Academic Press, 1978.

Viscosity effects on the behavior of a rising bubble

WANG, Han; ZHANG, Zhen yu; YANG, Yong ming; ZHANG, Hui sheng

01 longkai guo Page 1
15/2/2018 9:46

02 longkai guo Page 1
19/2/2018 15:23

03 longkai guo Page 1
19/2/2018 16:35

04 longkai guo Page 1
19/2/2018 16:36

05 longkai guo Page 1
19/2/2018 16:38

06 longkai guo Page 1
19/2/2018 16:41